Available online at www.sciencedirect.com
ScienceDirect
Bioorganic & Medicinal Chemistry 16 (2008) 94–99
Bioorganic & Medicinal Chemistry

Pyrene–perylene as a FRET pair coupled to the N2′-functionality of 2′-amino-LNA

Dorthe Lindegaard,[a] Andreas S. Madsen,[a] Irina V. Astakhova,[b] Andrei D. Malakhov,[b] B. Ravindra Babu,[a] Vladimir A. Korshun[b] and Jesper Wengel[a,*]

[a]*Nucleic Acid Center*[†]*, Department of Physics and Chemistry, University of Southern Denmark, Campusvej 55, DK-5230 Odense M, Denmark*
[b]*Shemyakin-Ovchinnikov Institute of Bioorganic Chemistry, Russian Academy of Sciences, Miklukho-Maklaya 16/10, Moscow 117997, Russia*

Received 5 October 2006; revised 23 November 2006; accepted 27 April 2007
Available online 3 May 2007

Abstract—Detection of nucleic acid hybridization via fluorescence resonance energy transfer (FRET) using pyren-1-ylmethyl and perylen-3-ylmethyl N2′-functionalized 2′-amino-LNA nucleosides incorporated into oligonucleotides exhibited a clear distance dependence of the FRET efficiency, ranging from below 10% when the fluorophores were approximately 40 Å apart to approximately 90% when the fluorophores were in close proximity.

1. Introduction

Fluorescence spectroscopy to monitor DNA hybridization using DNA labeled with fluorescent dyes is an established, straightforward, and relatively inexpensive technique. The fluorescent dyes can be bound either non-covalently to DNA[1,2] or DNA probes can be labeled with reporter groups.[3,4] In both situations the principle is to take advantage of a change in one or more fluorescent properties such as quantum yield, lifetime or fluorescence intensity upon hybridization with the target sequence. If different fluorophores are attached, the detection of nucleic acid hybridization via fluorescence resonance energy transfer (FRET) is possible. The majority of the donor–acceptor pairs used in FRET studies is structurally limited to being composed of one dye from the fluorescein family and another from the rhodamine family.[5,6] These dyes are often attached through a flexible linker, thereby enabling them to move freely in space in ways that may complicate the interpretation of the fluorescence measurements. Furthermore, as the fluorescent properties of fluorescein vary with changes in pH,[7] other fluorophores like aromatic hydrocarbons are of significant interest as means of expanding the field of application of FRET-based designs.[8,9]

One reported aromatic hydrocarbon FRET pair is based on pyrene as donor and perylene as acceptor.[9] Perylene has as spectral characteristics high quantum yield and spectral absorption overlap with the emission spectrum of pyrene allowing these two aromatic hydrocarbons to constitute a FRET pair. Only few reports on perylene attached to DNA have been published,[9–15] though the aromatic system has been widely used in studies of lipid derivatives as membrane probes[16–19] to, for example, follow the membrane packing and dynamics by fluorescence.[20]

Masuko and coworkers have studied pyrene and perylene as FRET pair when coupled to DNA, reporting a FRET efficiency approaching 100% when the two fluorophores were in close proximity upon DNA hybridization.[9] To further investigate this FRET pair and the influence of distance and position between the two fluorophores on FRET efficiency, we were interested in introducing the two dyes as N2′-functionalities of the thymine derivative of 2′-amino-LNA.[21] We anticipated that a short and relatively rigid linker would allow us to precisely arrange the two fluorophores at different positions along a duplex and thereby study how the

Keywords: Amino-LNA; Pyrene; Perylene; FRET.
[†] A research center funded by the Danish National Research Foundation for studies on nucleic acid chemical biology.
* Corresponding author. Tel.: +45 6550 2510; fax: +45 6612 8780; e-mail: jwe@ifk.sdu.dk

0968-0896/$ - see front matter © 2007 Elsevier Ltd. All rights reserved.
doi:10.1016/j.bmc.2007.04.056

distance between the two fluorophores would influence the FRET efficiency. In addition, we wanted to evaluate the effect of having the two fluorophores linked to nucleotides positioned, relatively to each other, either toward the 5′-ends or toward the 3′-ends of the two strands.

2. Results and discussion

Experimental details of the synthesis of phosphoramidite building blocks **1a** and **1b** will be reported elsewhere[22] (Scheme 1).

Six different ON sequences having monomer **X** positioned at different locations along the DNA strand were prepared using phosphoramidite **1a** (Table 1; **ON3**–**ON8**). Furthermore we utilized phosphoramidite **1b** to prepare two different complementary sequences having monomer **Y** positioned near either the 5′-end (Table 1; **ON9**) or the 3′-end (Table 1; **ON10**) to study if the energy transfer efficiency along the DNA:DNA duplex is preferred in one direction over the other.

Thermal denaturation experiments of modified duplexes revealed that the melting temperature (T_m value) was not affected significantly by incorporation of monomers **X** and **Y** relative to the unmodified reference duplex (ΔT_m values = +0.5 to +1.5 °C relative to **ON1**:**ON2**, Table 1). The only exception was a T_m value of 59.5 °C for duplex **ON4**:**ON10** corresponding to an increase of 5.0 °C relative to the reference duplex. This increase can be explained by a stabilizing perylene–pyrene interaction (supported by exciplex formation; data not shown). We have earlier observed a similar T_m value of a duplex having two pyrene units in an identical constitution.[23]

Steady-state fluorescence emission spectra of **ON3**–**ON8** as single strands or when hybridized with **ON2** revealed a typical pyrene monomer fluorescence spectrum with

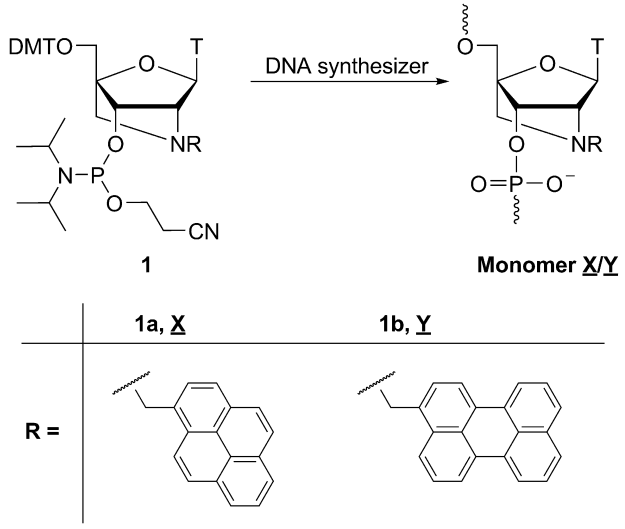

Scheme 1. Synthesis of oligonucleotides containing monomers **X** and **Y**.

λ_{max} at ~379 and ~398 nm upon excitation at 340 nm, whereas **ON9** and **ON10** as single strands or when hybridized to **ON1** displayed typical perylene monomer fluorescence emission bands with λ_{max} at ~451 and ~480 nm (and a shoulder at ~520 nm) upon excitation at 415 nm (data not shown).

We examined energy transfer from pyrene to perylene in the different duplexes (See Fig. 1). The steady-state fluorescence emission spectra showed two segments of structured emission bands upon excitation at 340 nm. The first segment was identical to the fluorescence monomer band derived from pyrene, the second portion matching the fluorescence monomer bands from perylene.

The FRET efficiencies (E_A) were determined by the equation

$$E_A = \frac{\varepsilon_A}{\varepsilon_D}\left(\frac{I_{AD}}{I_A} - 1\right),$$

where ε_A and ε_D are the molar extinction coefficients of the acceptor and donor at the excitation wavelength, and I_{AD} and I_A are the fluorescence intensities at the acceptor emission wavelength in the presence and absence of the donor, respectively. We calculated the FRET efficiencies (E_A values; Table 1) from pyrene to perylene and found these to be consistent with the trends observed in the fluorescence emission spectra (Fig. 1). We found that the FRET efficiency decreased dramatically when the number of base pairs between the donor and the acceptor was increased (Table 1, compare e.g., E_A for **ON8**:**ON9** and **ON7**:**ON9**). Furthermore, we observed a dependence on the relative arrangement of the two functionalized monomers within the duplex. FRET is more efficient when monomers **X** and **Y**, relative to each other, are positioned toward the 5′-end of the oligonucleotide to which they are linked (e.g., as in **ON6**:**ON9**), than when the functionalized monomers, relative to each other, are positioned toward the 3′-end of the oligonucleotide to which they are linked (e.g., as in **ON6**:**ON10**). In the set of duplexes formed by **ON3**, **ON4**, **ON5**, **ON6**, **ON7**, and **ON8** with **ON9** as complementary strand, the efficiencies were about 10% when monomers **X** and **Y** were 6–10 base pairs apart, increasing to approximately 90% when no base pairs were separating the monomers (**ON8**:**ON9**). The same high efficiency was observed for **ON3**:**ON10**, having the modified monomers in a similar constitution as in **ON8**:**ON9**. In the second set of duplexes, consisting of **ON4**, **ON5**, **ON6**, and **ON8** with **ON10** as the complementary strand, a trend was observed toward lower FRET efficiencies, decreasing from approximately 70% to below 10% as the number of base pairs between monomers **X** and **Y** was increased.

To further investigate the observed trends in FRET efficiency a series of simple force field calculations was performed. Standard B-type duplexes were modified with monomers **X** and **Y** and subjected to molecular dynamics simulation and minimization using the AMBER force field as implemented in MacroModel V9.1.[24] In all cases the lowest energy structure showed the

Table 1. Thermal denaturation and FRET efficiency studies[a]

#	Sequences (duplexes)	T_m (°C)	E_A (%)
ON1 **ON2**	5′-GAA CGT ATA TAT ATA TAG CAC G 3′-CTT GCA TAT ATA TAT ATC GTG C	54.5 (Ref.)	—
ON3 **ON9**	5′-GAA CG**X** ATA TAT ATA TAG CAC G 3′-CTT GCA TAT ATA TAT A**Y**C GTG C	56.0	10
ON4 **ON9**	5′-GAA CGT A**X**A TAT ATA TAG CAC G 3′-CTT GCA TAT ATA TAT A**Y**C GTG C	56.0	13
ON5 **ON9**	5′-GAA CGT ATA **X**AT ATA TAG CAC G 3′-CTT GCA TAT ATA TAT A**Y**C GTG C	56.0	13
ON6 **ON9**	5′-GAA CGT ATA TA**X** ATA TAG CAC G 3′-CTT GCA TAT ATA TAT A**Y**C GTG C	56.0	26
ON7 **ON9**	5′-GAA CGT ATA TAT A**X**A TAG CAC G 3′-CTT GCA TAT ATA TAT A**Y**C GTG C	56.0	58
ON8 **ON9**	5′-GAA CGT ATA TAT ATA **X**AG CAC G 3′-CTT GCA TAT ATA TAT A**Y**C GTG C	56.0	89
ON3 **ON10**	5′-GAA CG**X** ATA TAT ATA TAG CAC G 3′-CTT GCA **Y**AT ATA TAT ATC GTG C	55.0	87
ON4 **ON10**	5′-GAA CGT A**X**A TAT ATA TAG CAC G 3′-CTT GCA **Y**AT ATA TAT ATC GTG C	59.5	67[b]
ON5 **ON10**	5′-GAA CGT ATA **X**AT ATA TAG CAC G 3′-CTT GCA **Y**AT ATA TAT ATC GTG C	56.0	25
ON6 **ON10**	5′-GAA CGT ATA TA**X** ATA TAG CAC G 3′-CTT GCA **Y**AT ATA TAT ATC GTG C	56.0	10
ON8 **ON10**	5′-GAA CGT ATA TAT ATA **X**AG CAC G 3′-CTT GCA **Y**AT ATA TAT ATC GTG C	55.5	7

[a] Thermal denaturation temperatures (T_m values) were determined at a concentration of 1.5 μM of the two complementary strands in a medium salt buffer (100 mM NaCl, 0.1 mM EDTA and pH 7.0 adjusted with 10 mM NaH_2PO_4/5 mM Na_2HPO_4). FRET efficiencies (E_A values) were calculated with respect to the acceptor from the molar extinction coefficients and the relative intensity in the excitation spectrum at 340 nm.

[b] The perylene monomer fluorescence was shifted to longer wavelength.

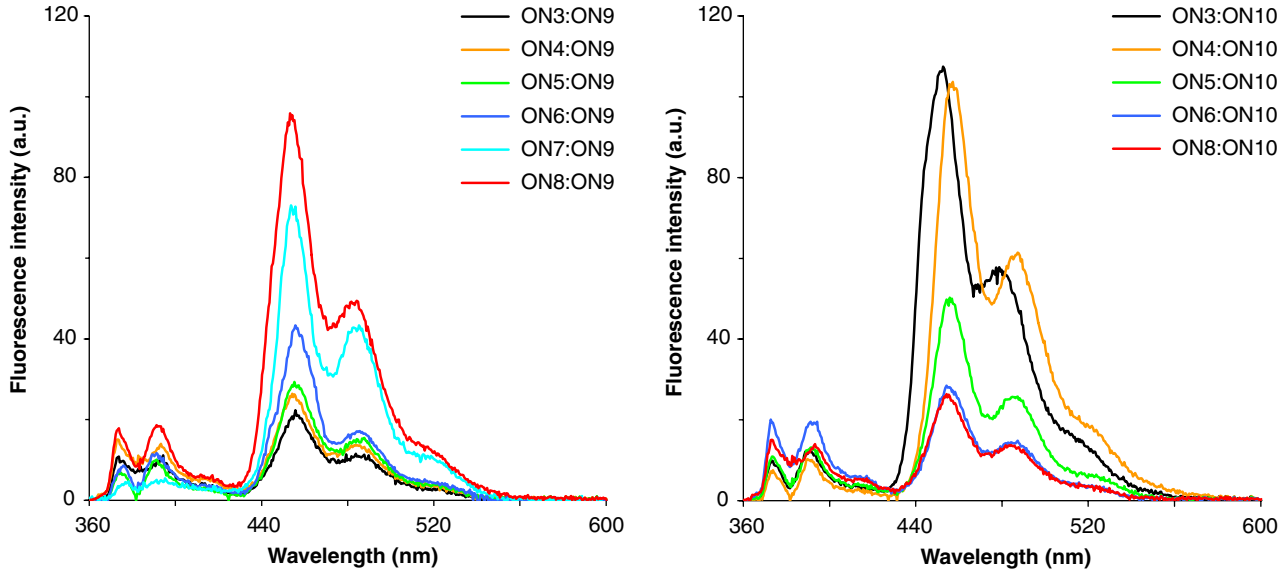

Figure 1. Steady-state fluorescence emission spectra were recorded in a medium salt buffer (100 mM NaCl, 0.1 mM EDTA and pH 7.0 adjusted with 10 mM NaH_2PO_4/5 mM Na_2HPO_4) with excitation at 340 nm at 19 °C. The concentration of the ONs was 0.15 μM.

functionalities to be positioned in the minor groove of the duplex, following the helical curvature of the groove, and in all cases, except **ON4**:**ON10**, the individual fluorophores were oriented toward the 3′-end of the oligonucleotide to which they were linked. As a result, the fluorophores of duplexes consisting of **ON3**, **ON4**, **ON5**, **ON6**, **ON7**, and **ON8** with **ON9** as complementary strand, as well as **ON3**:**ON10**, are oriented toward

each other, whereas the fluorophores of duplexes **ON5**:**ON10**, **ON6**:**ON10**, and **ON8**:**ON10** are oriented away from each other (see Fig. 2 for representative structures). In the lowest energy structure of **ON4**:**ON10** the perylene moiety was found to be oriented toward the 5′-end of the oligonucleotide to which it is linked, resulting in both fluorophores pointing toward the same end of the duplex.

The distance between the two fluorophores was found to range from approximately 40 Å (**ON3**:**ON9**) to approximately 10 Å (**ON8**:**ON9**), and a clear distance dependence of the FRET efficiency was found, testified by a gradual increase when the distance was decreased (see Fig. 3). However, the observed change in FRET efficiency is evidently not purely a distance effect, but apparently also, as already indicated, a result of the relative position of the two fluorophores within the two strands constituting the duplex. Thus, the observed FRET is more efficient when the two fluorophores are arranged to point toward each other rather than when arranged to point away from each other.

We suggest that the observed difference in FRET efficiency is a consequence of restricting the orientation, and thereby the dipole moments, of the two fluorophores. Since FRET is a distance-dependent relation of the two transient dipole moments,[10,25] this is expected to have great impact on the FRET efficiency. However, even though functionalities of 2′-amino-LNA are precisely positioned within the minor groove of the duplex, we still anticipate some degree of freedom with respect to the orientation of the fluorophores. Furthermore, it is known that the LNA-skeleton is conformationally driving the local duplex geometry from B-type towards an intermediate A/B-type duplex.[26] No attempts were made to take this conformational change into account during the modeling protocol. As a result, assignment of the involved dipole vectors is not as straightforward as in end-capped systems,[10] where the two fluorophores are kept at well-defined positions by covalent linkages and by π-π stacking with the adjacent nucleobases. A deeper insight into the precise structural features of our system would demand thorough structural studies which are beyond the scope of this investigation.

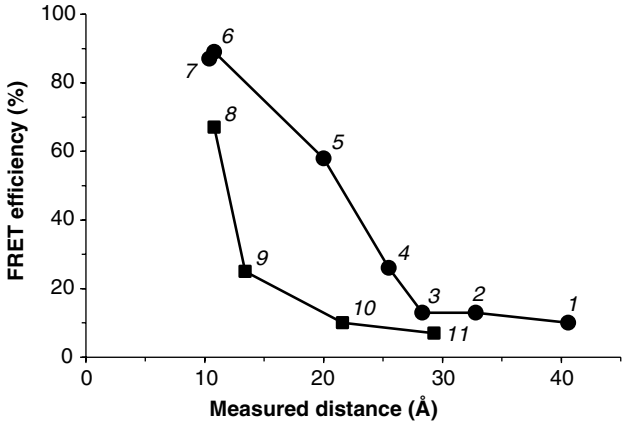

Figure 3. FRET efficiency as a function of the distance between the fluorophores. **ON3**:**ON9** (1); **ON4**:**ON9** (2); **ON5**:**ON9** (3); **ON6**:**ON9** (4); **ON7**:**ON9** (5); **ON8**:**ON9** (6); **ON3**:**ON10** (7); **ON4**:**ON10** (8); **ON5**:**ON10** (9); **ON6**:**ON10** (10); **ON8**:**ON10** (11).

3. Conclusion

In conclusion the attachment of pyrene and perylene as N2′-functionalities of 2′-amino-LNA nucleotide monomers and incorporation of these in the two complementary strands of 22-mer DNA duplexes resulted in very high FRET efficiencies (approximately 90%) when the two fluorophores were in close proximity. A gradual decrease in FRET efficiency was observed as the distance between the two fluorophores was increased, though FRET was observed also for duplexes having the two fluorophores separated by 10 unmodified base pairs. Furthermore, data even for duplexes resulting in low efficiencies due to separation of the two dyes were still straightforward to interpret as a result of the high fluorescence quantum yield of perylene. This confirms that pyrene–perylene is an excellent donor–acceptor pair, also when attached to 2′-amino-LNA monomers. The results obtained represent a step forward toward the development of advanced FRET systems along DNA duplexes for diagnostic applications.

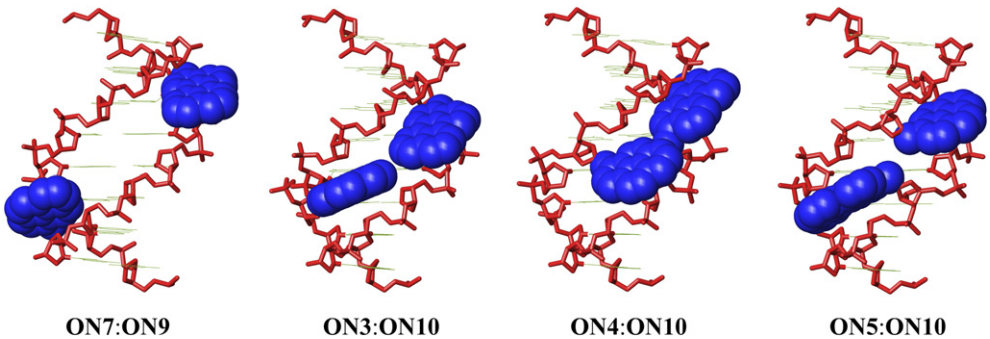

Figure 2. Truncated representations of the lowest energy structure obtained from molecular modeling of **ON7**:**ON9**, **ON3**:**ON10**, **ON4**:**ON10**, and **ON5**:**ON10**, respectively. Hydrogens, sodium ions, and bond orders have been omitted for clarity. Coloring scheme: nucleobases, green; sugar-phosphate backbone, red; pyren-1-ylmethyl and perylen-3-ylmethyl moieties, blue.

4. Experimental

4.1. Synthesis of modified oligonucleotides

Synthesis of ONs containing monomers **X** and **Y** was performed in 0.2 μmol scale on an Applied Biosystems Expedite automated DNA synthesizer using commercially available β-cyanoethoxy phosphoramidites. Standard procedures (2 min coupling time, 1*H*-tetrazole as catalyst) were used except for extended coupling times (10 min) for phosphoramidites **1a** and **1b**, resulting in stepwise coupling yields of ~98% for **1a** and **1b** and >99% of unmodified DNA phosphoramidites. Removal of protecting groups and cleavage from solid support was effected using 32% aq ammonia for 16 h at 55 °C. The ONs were purified to a purity of >80% on a Waters Prep LC 4000 system equipped with a Xterra MS C18-column (10 μm, 300 mm × 7.8 mm) using an isocratic hold of 100% A-buffer for 5 min followed by a linear gradient to 55% B-buffer over 75 min at a flow rate of 1.0 mL/min (A-buffer: 95% 0.1 M aq NH_4HCO_3, 5% CH_3CN; B-buffer: 25% 0.1 M aq NH_4HCO_3, 75% CH_3CN). Subsequently, the ONs were detritylated (80% aq AcOH, 20 min) and either precipitated (abs EtOH, −18 °C, 12 h) and washed with abs EtOH or desalted by RP-HPLC using the system mentioned above except for using an isocratic hold of 100% A-buffer for 4 min followed by a linear gradient to 100% B-buffer over 11 min at a flow rate of 2.5 mL/min. Composition of ONs was verified by MALDI-MS analysis, *m*/*z* ($[M-H]^-$, found/calcd): **ON3**, 7007/7007; **ON4**, 7003/7007; **ON5**, 7007/7007; **ON6**, 7016/7007; **ON7**, 7011/7007; **ON8**, 7009/7007; **ON9**, 6988/6990; **ON10**, 6993/6990.

4.2. Thermal denaturation studies

Concentrations of ONs were calculated using the following extinction coefficients ($OD_{260}/mol^{-1}\,cm^{-1}$): G—12010; A—15200; T/U—8400; C—7050. For the pyrene and perylene units an extinction coefficient ($OD_{260}/mol^{-1}\,cm^{-1}$) of 20000 was added. Thermal denaturation temperatures (T_m values) were measured on a Perkin-Elmer Lambda 35 UV/vis spectrometer equipped with a PTP-6 Peltier temperature programmer and determined as the maximum of the first derivative of the thermal denaturation curve (A_{260} vs temperature). Thermal denaturation studies were recorded in medium salt phosphate buffer (100 mM NaCl, 0.1 mM EDTA and pH 7.0 adjusted with 10 mM NaH_2PO_4/5 mM Na_2HPO_4). ONs (1.5 μM concentration of each strand) were thoroughly mixed, denatured by heating to 90 °C, and subsequently cooled to the starting temperature of the experiment. The absorbance was measured at 0.5 °C intervals using 1 mL quartz optical cells with a pathlength of 1.0 cm. The temperature of the denaturation experiments ranged from at least 15 °C below T_m to 15 °C above T_m. A temperature ramp of 0.5 °C/min was used. Reported thermal denaturation temperatures are an average of at least two measurements within ±0.5 °C.

4.3. Fluorescence steady-state emission studies

The fluorescence studies were carried out on a Perkin-Elmer LS 55 luminescence spectrometer equipped with a Peltier temperature controller. ON concentrations were 0.15 μM of each strand and the strands were thoroughly mixed, denatured by heating to 90 °C, and subsequently cooled to 19 °C. Quarts cuvettes with a path length of 1.0 cm were used. The fluorescence studies were carried out at 19 °C in a medium salt buffer (100 mM NaCl, 0.1 mM EDTA and pH 7.0 adjusted with 10 mM NaH_2PO_4/5 mM Na_2HPO_4). Corrections were made for solvent background but no attempts were made to eliminate dissolved oxygen in the buffer since control experiments, in which N_2 was bubbled through the buffer solution for 30 min, did not change the overall fluorescence emission. The steady-state fluorescence emission spectra were obtained as an average of five scans using the excitation wavelength noted in each experiment with an excitation slit of 4.0 nm, an emission slit of 2.5 nm, and a scan speed of 120 nm/min.

4.4. Molecular modeling

Duplex **ON1**:**ON2** was built having standard B-type helical geometry and subsequently modified to the duplexes of interest in MacroModel V9.1.[24] The charge of the phosphodiester backbone was neutralized with sodium ions, which were placed 3.0 Å from the two non-bridging oxygen atoms. During the following molecular dynamics simulation and minimization, the sodium–oxygen distances were restrained to 3.0 Å by a force constant of 100 kJ/mol Å^2. All atoms except the adjacent phosphodiester groups (including C3′ of the preceding nucleotide, and C5′, 2 × H5′, and C4′ of the following nucleotide) and the sugar and fluorophore moieties of monomers **X** and **Y** were frozen, and the duplex was minimized using the Polak–Ribiere conjugate gradient method, the all-atom AMBER force field,[27,28] and GB/SA solvation model[29] as implemented in MacroModel V9.1. Non-bonded interactions were treated with extended cut-offs (van der Waals 8.0 Å and electrostatics 20.0 Å). The minimized structures were then (using the same constraints as described above) submitted to 3 ns of stochastic dynamics (simulation temperature 300 K, time step 2.2 fs, SHAKE all bonds to hydrogen), during which 300 structures were sampled and subsequently minimized. Distances between fluorophores were determined as the distance between the center of the pyrene and perylene units.

Acknowledgments

We greatly appreciate funding from The Danish National Research Foundation, Villum Kann Rasmussen Fonden, and The Oticon Foundation. I.V.A., A.D.M., and V.A.K. acknowledge support of RFBR Grant 06-03-32426.

References and notes

1. Xu, Z.; Bai, G.; Dong, C. *Bioorg. Med. Chem.* **2005**, *13*, 5694.
2. Harrisman, W. O.; Wabl, M. *Anal. Biochem.* **1995**, *228*, 336.
3. Johansson, M. K.; Cook, R. M. *Chem. Eur. J.* **2003**, *9*, 3466.
4. Piestert, O.; Barsch, H.; Buschmann, V.; Heinlein, T.; Knemeyer, J. P.; Weston, K. D.; Sauer, M. *Nano Lett.* **2003**, *3*, 979.
5. Rist, M. J.; Marino, J. P. *Curr. Org. Chem.* **2002**, *6*, 775.
6. Marras, S. A. E.; Kramer, F. R.; Tyagi, S. *Nucleic Acids Res.* **2002**, *30*, e122.
7. Martin, M. M.; Lindquist, L. J. *J. Luminescence* **1975**, *10*, 381.
8. Malakhov, A. D.; Skorobogatyi, M. V.; Prokhorenko, I. A.; Gontarev, S. V.; Kozhich, D. T.; Stetsenko, D. A.; Stepanova, I. A.; Shenkarev, Z. O.; Berlin, Y. A.; Korshun, V. A. *Eur. J. Org. Chem.* **2004**, 1298.
9. Masuko, M.; Ohuchi, S.; Sode, K.; Ohtani, H.; Shimadzu, A. *Nucleic Acids Res.* **2000**, *28*, e34.
10. Lewis, F. D.; Zhang, L.; Zuo, X. *J. Am. Chem. Soc.* **2005**, *127*, 10002.
11. Wang, W.; Li, L. S.; Helms, G.; Zhou, H. H.; Li, A. D. Q. *J. Am. Chem. Soc.* **2003**, *125*, 1120.
12. Balakin, K. V.; Korshun, V. A.; Mikhalev, I. I.; Maleev, G. V.; Malakhov, A. D.; Prokhorenko, I. A.; Berlin, Y. A. *Biosens. Bioelectron.* **1998**, *13*, 771.
13. Zheng, Y.; Long, H.; Schatz, G. C.; Lewis, F. D. *Chem. Commun.* **2005**, 4795.
14. Aubert, Y.; Asseline, U. *Org. Biomol. Chem.* **2004**, *2*, 3496.
15. Koval, V. V.; Pyshnyi, D. V.; Fedorova, O. S. *J. Biomol. Struct. Dyn.* **2001**, *19*, 515.
16. Sandonella, G.; Haalck, L.; Spener, F.; Faber, K.; Paltauf, F.; Hermetter, A. *Chirality* **1998**, *8*, 481.
17. Lakowicz, J. R.; Knutson, J. R. *Biochemistry* **1980**, *19*, 905.
18. Kawato, S.; Kinosita, K.; Ikegami, A. *Biochemistry* **1977**, *16*, 2319.
19. Bagatolli, L. A.; Gratton, E. *J. Fluoresc.* **2001**, *11*, 141.
20. Khan, T. K.; Parkson, L. C. *Biophys. J.* **2000**, *78*, 1390.
21. Singh, S. K.; Kumar, R.; Wengel, J. *J. Org. Chem.* **1998**, *63*, 10035.
22. Babu, B. R.; Lindegaard, D.; Kumar, T. S.; Astakhova, I. V.; Malakov, A. D.; Sørensen, M. D.; Korshun, V. A.; Hrdlicka, P. J.; Wengel, J. In preparation.
23. Hrdlicka, P. J.; Babu, B. R.; Sørensen, M. D.; Wengel, J. *Chem. Commun.* **2004**, 1478.
24. MacroModel, version 9.1, Schrödinger, LLC, New York, NY, 2005.
25. Förster, T. *Ann. Phys.* **1948**, *2*, 55.
26. Nielsen, K. E.; Singh, S. K.; Wengel, J.; Jacobsen, J. P. *Bioconjugate Chem.* **2000**, *11*, 228–238.
27. Weiner, S. J.; Kollman, P. A.; Case, D. A.; Singh, U. C.; Ghio, C.; Alagona, G.; Profeta, S.; Weiner, P. *J. Am. Chem. Soc.* **1984**, *106*, 765.
28. Weiner, S. J.; Kollman, P. A.; Nguyen, D. T.; Case, D. A. *J. Comput. Chem.* **1986**, *7*, 230.
29. Still, W. C.; Tempczyk, A.; Hawley, R. C.; Hendrickson, T. *J. Am. Chem. Soc.* **1990**, *112*, 6127.